THE JOURNAL OF PHYSICAL CHEMISTRY Letters

Letter

pubs.acs.org/JPCL

Extended Law of Corresponding States Applied to Solvent Isotope Effect on a Globular Protein

Saskia Bucciarelli,[†] Najet Mahmoudi,[*,†,‡] Lucía Casal-Dujat,[†] Marie Jéhannin,[†] Corinne Jud,[‡] and Anna Stradner[*,†]

[†]Physical Chemistry, Department of Chemistry, Lund University, SE-22100 Lund, Sweden

[‡]Adolphe Merkle Institute (AMI), University of Fribourg, CH-1700 Fribourg, Switzerland

Supporting Information

ABSTRACT: Investigating proteins with techniques such as NMR or neutron scattering frequently requires the partial or complete substitution of D_2O for H_2O as a solvent, often tacitly assuming that such a solvent substitution does not significantly alter the properties of the protein. Here, we report a systematic investigation of the solvent isotope effect on the phase diagram of the lens protein γB-crystallin in aqueous solution as a model system exhibiting liquid−liquid phase separation. We demonstrate that the observed strong variation of the critical temperature T_c can be described by the extended law of corresponding states for all H_2O/D_2O ratios, where scaling of the temperature by T_c or the reduced second virial coefficient accurately reproduces the binodal, spinodal, and osmotic compressibility. These findings highlight the impact of H_2O/D_2O substitution on γB-crystallin properties and warrant further investigations into the universality of this phenomenon and its underlying mechanisms.

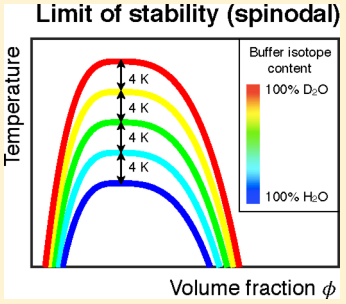

Since its first production by Lewis and MacDonald in 1933 and despite its low natural availability (at one part in about 6500 parts of light water),[1] heavy water (D_2O) and its biological effects have been investigated extensively.[2] Studies included, for example, the cytotoxic and cytostatic activities of D_2O against human cancer cells,[3] its contradictory effects on cellular secretion,[4] and the absence of retinal toxicity when D_2O is used in bovine and human retina perfusion studies.[5] Furthermore, solvent isotope effects in protein studies have contributed to a deeper understanding of protein structural stability. Indeed, secondary structure studies of disparate proteins have shown that the folded state is mostly stabilized in D_2O.[6−11] Additionally, D_2O was shown to increase protein stability against thermal denaturation.[12−14]

Some experimental techniques, such as nuclear magnetic resonance (NMR), spectroscopic techniques,[15,16] and neutron scattering,[17,18] commonly used to investigate protein internal and solution structure and dynamics often rely on solvent isotope substitution, partially or completely replacing H_2O by D_2O. In coherent neutron scattering methods, deuterium is used instead of hydrogen in order to decrease the background arising from the incoherent scattering of the latter or to perform contrast variation studies on multicomponent systems.[19] In infrared spectroscopy,[15] vibrational circular dichroism[20] and NMR,[21] the signal from water absorption bands interferes considerably with that from protein molecules, thus making the use of a deuterated solvent necessary. In interpreting the results of such measurements, the effects of solvent isotope on protein colloidal stability are frequently left out and it is often assumed that proteins have essentially the same solution structure in H_2O and D_2O. Earlier work, however, has shown that lysozyme, a globular protein with a short-range attractive interaction potential, is less soluble in D_2O than in H_2O,[22,23] which is linked to enhanced protein−protein attractions in D_2O.[24] Stradner et al.[25] found that using D_2O as solvent for lysozyme strongly affects its colloidal stability. Additionally, the effect of isotope substitution on solvent properties, and consequently on interactions and phase behavior in other colloidal systems such as polymer solutions and surfactant systems, is also well established.[19] This clearly calls for an in-depth investigation of the effect of solvent isotope content on the phase behavior and interaction potential governing solutions of globular proteins, in order to help clarify to which extent results obtained in solvents with different isotope content can be compared and used to draw conclusions on living systems, such as cells or the eye lens, which contain only H_2O. We have therefore performed a systematic study of the phase behavior and the solution structure of the globular protein γB-crystallin, one of the major components of the eye lens, in aqueous solutions of varying deuterium content.

γB-crystallin, the smallest of the eye lens proteins with a radius of about 1.8 nm is commonly used as a model system for colloidal particles interacting via a short-range attractive interaction potential.[26] It displays a complex phase behavior that combines liquid−liquid phase separation and dynamical arrest[27−29] with an arrest line that extends into the unstable region below the spinodal, a feature previously also observed in lysozyme.[30] The equilibrium phase diagram of the latter was

Received: March 14, 2016
Accepted: April 14, 2016
Published: April 14, 2016

DOI: 10.1021/acs.jpclett.6b00593
J. Phys. Chem. Lett. 2016, 7, 1610−1615

shown to follow the extended law of corresponding states (ELCS) of Noro and Frenkel,[31] whereby the critical point and the connected coexistence curve at various ionic strengths are rescaled using the reduced second virial coefficient b_2, defined as the ratio of the second virial coefficient B_2 and $B_2^{HS} = 2\pi\sigma^3/3$, the second virial coefficient of a solution of hard spheres with the same diameter σ as the protein. This demonstrates that the critical point and the coexistence curve of lysozyme depend on the integral features of its interaction potential and not on the details of the latter.[32,33] Moreover, Gripon et al.[22] reported that in a salt-concentration range of 0.3−0.6 M NaCl, increasing the concentration of NaCl by 0.1 M was found to have the same effect on the solubility of lysozyme as substituting H_2O by D_2O.[22] We may thus speculate that the ELCS applies not only to globular proteins in solutions with different ionic strength but also to solvents with varying hydrogen isotope content.

In this study, we investigate the effect of the gradual substitution of D_2O for H_2O in γB-crystallin solutions on their phase behavior and the strength of their interaction potential. We show, through a combination of transmission measurements, static light scattering (SLS), and small-angle X-ray scattering (SAXS), that increasing the D_2O content of the solvent has a large effect on both and that the validity of the ELCS can indeed be extended to H_2O/D_2O substitution.

We located the metastable binodal (or coexistence curve for liquid−liquid phase separation) and the spinodal of γB-crystallin solutions in five different solvents with varying H_2O/D_2O content (cf. Table 1, cf. Supporting Information (SI) for details). The resulting data is shown in Figure 1a and b. The critical temperature T_c is clearly strongly affected by the amount of deuterium in the solution, as summarized in the inset of Figure 1. Fitting the left ($\phi < \phi_c$) and right ($\phi > \phi_c$) branches of all binodals and spinodals with

$$T = T_c\left[1 - A\left(\frac{|\phi - \phi_c|}{\phi_c}\right)^{1/\beta}\right] \quad (1)$$

with individual fitting parameters A and a critical exponent $\beta = 0.33$,[29] we find that ϕ_c on the other hand remains unaffected by D_2O and that the shape of the curves does not depend on solvent isotope content. In fact, the same fitting parameters $A_{b,left} = (0.06 \pm 0.02)$ and $A_{b,right} = (0.02 \pm 0.01)$ reproduce all the binodals and the same $A_{s,left} = (0.39 \pm 0.08)$ and $A_{s,right} = (0.08 \pm 0.04)$ reproduce all the spinodals (cf. Figure 1a and b). This becomes even more apparent when scaling the temperature by T_c, which causes the curves to superimpose, as shown in Figure 1c and d, reminiscent of the results reported by Gibaud et al.[32] and by Platten et al.[33] for lysozyme in solutions with varying ionic strength. These authors have shown that under these conditions, the Noro−Frenkel ELCS applies and that the reduced second virial coefficient b_2 can be used to predict the phase behavior of the protein. To test whether the isotope effect on the phase behavior of γB-crystallin can also be predicted based on the ELCS, we have experimentally determined B_2 from SLS on dilute solutions in 100/0, 50/50, and 0/100 solvent, following the method described by Gibaud et al.[32] (cf. SI for details). The resulting temperature-dependent b_2 values are shown in Figure 2a. At the critical temperature T_c, we find $b_2(T_c) = -2.7 \pm 0.5$ for all three solutions under investigation. When scaled to T_c, all b_2 indeed fall onto one master curve, as shown in Figure 2b. We discuss the following results in light of a simple square-well (SW) potential

$$U_{SW}(r) = \begin{cases} \infty & r < \sigma \\ -\varepsilon & \sigma \le r \le \Lambda\sigma \\ 0 & r > \Lambda\sigma \end{cases} \quad (2)$$

describing the interactions as a combination of a hard core repulsion and a short-range attraction of strength (or well depth) ε and range Λ. In accordance with earlier results,[29,30] we take $\Lambda = 1.20$, that is, a range of the attractive interaction potential corresponding to 20% of the protein diameter. b_2 is then given by

$$b_2(T^*) = 1 - (\Lambda^3 - 1)\left(\exp\frac{1}{T^*} - 1\right) \quad (3)$$

where $T^* = k_BT/\varepsilon$.[33] Following the approach of Platten et al.,[33] we assume a linear dependence of the SW depth on temperature and fit $b_2(T/T_c)$ with

$$b_2\left(\frac{T}{T_c}\right) = 1 - (\Lambda^3 - 1)\left[\exp\left(\frac{aT/T_c + b}{T/T_c}\right) - 1\right] \quad (4)$$

The fitting parameters a and b were found to be $a = -3.3 \pm 0.5$ and $b = 5.0 \pm 0.5$. Combining eqs 3 and 4, we obtain the depth of the SW as a function of T/T_c

$$\frac{\varepsilon}{k_BT} = \frac{aT/T_c + b}{T/T_c} \quad (5)$$

as shown in Figure 2c. Using eq 4, temperatures can universally be converted to b_2 and vice versa, as demonstrated in Figure 1c−f, where the binodals and spinodals obtained in all solvents superimpose when plotted in the $T/T_c-\phi$ plane, as well as in the $b_2-\phi$ plane. The ELCS proposed by Noro and Frenkel,[31] thus, can indeed accurately reproduce the phase diagram of this globular protein in solutions with different hydrogen isotope content.

To further investigate the validity of the ELCS, we now focus on $S^{-1}(0)$, the inverse static structure factor in the forward direction, related to the osmotic compressibility κ_T of the solution. We extracted $S^{-1}(0)$ from SAXS data, following the method described in an earlier publication.[29] Examples of static structure factors $S(q)$ for samples close to ϕ_c in 100/0, 50/50, and 0/100 solvents are given in Figure 3a−c, respectively. The critical (low-q) parts of the structure factors over a wide range of volume fractions were fitted with the OZ equation

$$S(q, T, \phi) = \frac{S_{crit}(0)}{1 + q^2\xi_s^2} + S_{non\text{-}crit} \quad (6)$$

which is the sum of a strongly temperature-dependent critical component ($S_{crit}(0)/(1 + q^2\xi_s^2)$), associated with the short-range attractions, and a temperature-independent noncritical background ($S_{non\text{-}crit}$), assumed to be q-independent in the low-q range ($q \ll q^*$) considered here.[34] As shown in Figure 4c, the

Table 1. Mixing Ratios of H_2O and D_2O Used in This Study and Corresponding Data Symbols Used in the Graphs

ratio	vol % H_2O	vol % D_2O	data symbol
100/0	100	0	green △
75/25	75	25	pink ▽
50/50	50	50	blue □
25/75	25	75	orange ◇
0/100	0	100	purple ○

DOI: 10.1021/acs.jpclett.6b00593
J. Phys. Chem. Lett. 2016, 7, 1610−1615

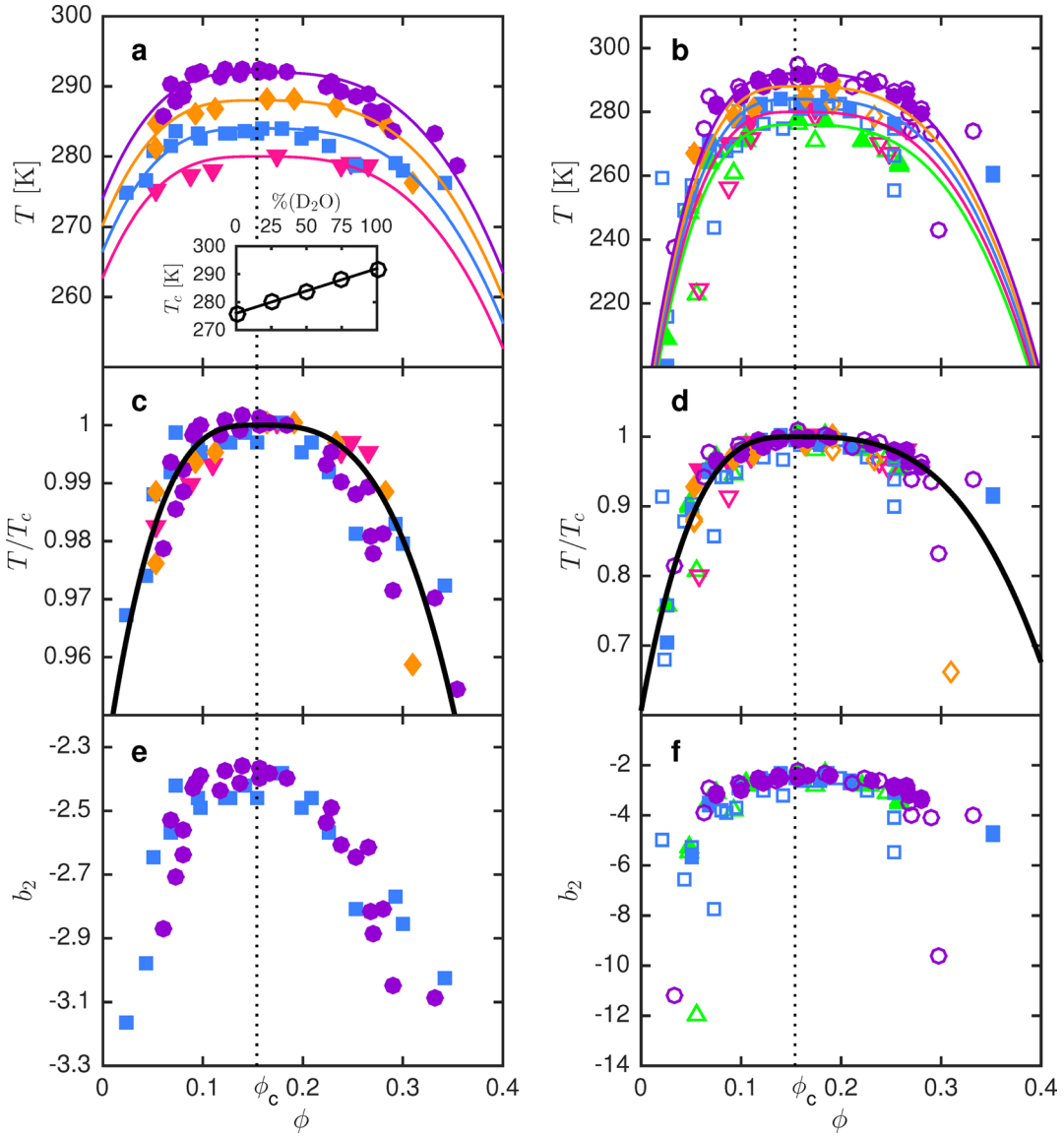

Figure 1. Binodal (left) and spinodal (right) of γB-crystallin solutions in solvents with varying hydrogen isotope content. (a) and (b) Unscaled data. (c) and (d) Data from (a) and (b) scaled by T_c. (e) and (f) Binodals and spinodals in the b_2–ϕ plane, where b_2 is the reduced second virial coefficient. The solid lines show the fits to eq 1 and the dotted line marks ϕ_c. Right: filled symbols correspond to T_{sp} from Ornstein–Zernike (OZ) fits to SAXS structure factors (eq 6) and open symbols correspond to T_{sp} from SLS. Inset: T_c of γB-crystallin solutions as a function of solvent D_2O content.

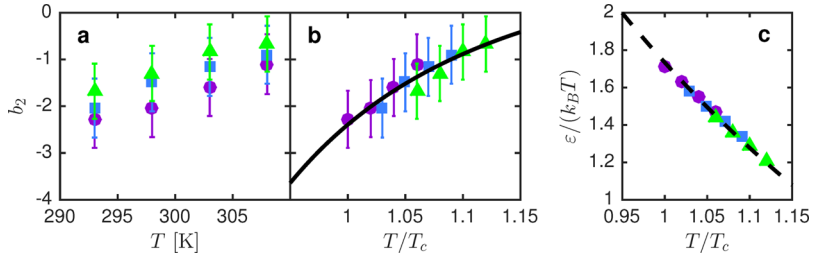

Figure 2. Reduced second virial coefficient b_2 of γB-crystallin in solvents with varying deuterium content, (a) as a function of temperature and (b) scaled by T_c. The solid black line shows the global fit (eq 4) to all data sets. (c) Well depth $\varepsilon/(k_BT) = 1/T^*$ of the SW potential as a function of reduced temperature. The dashed black line corresponds to eq 5.

latter follows the Carnahan–Starling (CS) prediction for $S(0)$ of hard spheres, that is, it is associated with the hard sphere interactions of the proteins. Moreover, all data points superimpose without further scaling, confirming that the hard core repulsion of the protein remains unaffected by solvent isotope substitution. $S_{crit}(0) = S_0\tau^{-\gamma}$, shown in Figure 4b, is the critical component of the static structure factor in the forward direction and $\xi_s = \xi_{s,0}\tau^{-\nu}$ is the static correlation length that

DOI: 10.1021/acs.jpclett.6b00593
J. Phys. Chem. Lett. 2016, 7, 1610–1615

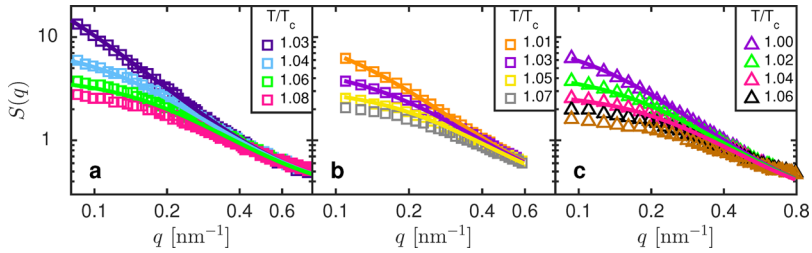

Figure 3. Critical part of the experimentally determined static structure factors $S(q)$ (data symbols) at $\phi = 0.16$ (close to ϕ_c) in (a) 100/0, (b) 50/50, and (c) 0/100 solvents, together with the OZ fits to the critical parts of the static structure factors close to criticality (eq 6, lines) at varying T/T_c.

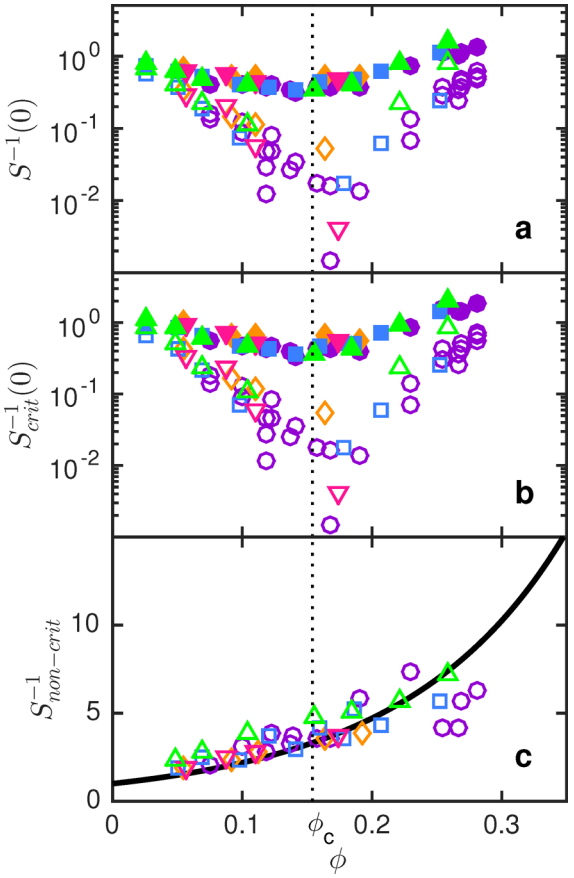

Figure 4. (a) $S^{-1}(0)$ obtained from SAXS (from OZ fits) for different solvent isotope content, scaled by T_c and (b) critical component $S^{-1}_{crit}(0)$, scaled by T_c at $T/T_c \approx 1.06$ (filled symbols) and $T/T_c \approx 1$ (open symbols). (c) Noncritical, T-independent background of $S(0)$. Also shown is the CS prediction for hard spheres (solid black line). The dotted line marks ϕ_c. Cf. Figure S2 in the SI for 3D plots of (a) and (b) containing the full data set over a large range of T/T_c.

measures the characteristic length scale of density fluctuations caused by critical phenomena. $\nu = 0.63$ and $\gamma = 1.24$ are the critical exponents from the Ising universality class[35,36] and $\tau = (T - T_{sp})/T_{sp}$ is the reduced temperature. This allows us to extract the spinodal temperature T_{sp} from OZ fits to $S(q)$ at each ϕ using S_0, $\xi_{s,0}$, T_{sp}, and $S_{non\text{-}crit}$ as fitting parameters and simultaneously fitting the structure factors at all measured T close to criticality with eq 6 (lines in Figure 3). We then find an average value of $\xi_{s,0} = (7.01 \pm 0.74)$ nm for the five solvents, independently of ϕ, which is in agreement with the value of (7.27 ± 0.71) nm found in pure D_2O solvent.[29] Moreover, the thus obtained T_{sp} values (filled symbols on the right-hand side of Figure 1) closely follow the spinodal obtained from SLS (open symbols). We now focus on low q values and thus length scales significantly larger than the protein size, that is, on the total forward structure factor $S(0) = S_{crit}(0) + S_{non\text{-}crit}$, shown in Figure 4a for the five hydrogen isotope contents investigated at two different temperatures scaled by T_c. $S^{-1}(0)$ exhibits a minimum around ϕ_c for a given temperature, due to the critical component, which also exhibits a minimum at the same ϕ (cf. Figure 4b). More importantly, the T_c-scaling causes $S^{-1}(0)$ and $S^{-1}_{crit}(0)$ corresponding to the different solvents to superimpose, similarly to the phase diagram. The ELCS, using T/T_c (or b_2) as a scaling parameter thus also applies to the osmotic compressibility.

In summary, the phase boundaries for liquid−liquid phase separation and the osmotic compressibility of aqueous solutions of the short-range attractive globular protein γB-crystallin scale with the reduced second virial coefficient b_2, quantifying protein−protein interactions, through the extended law of corresponding states (ELCS). This thermodynamic scaling confirms the applicability of the ELCS to the equilibrium properties of colloids with short-range attractions[32,37] and provides an extension of its predictive power to systems with varying hydrogen isotope content. Using a simple square-well (SW) fluid analysis, we moreover show that the well depth, a measure of the strength of the attractions, increases by about $0.26-0.27 k_B T$ when exchanging hydrogen for deuterium in the solvent. This proves that the isotope content of the solvent indeed has a dramatic effect on the protein interactions inducing a shift in critical temperature T_c of 16 K between pure H_2O and pure D_2O. This value is noticeably larger than the shift reported in the transition (or denaturation) temperature T_m of globular proteins, which is 2−6 K when D_2O is substituted for H_2O in the solvent.[10,13] Gripon et al.[24] reported a shift in the value of the second virial coefficient, as well as in the solubility of lysozyme in H_2O compared to D_2O, corresponding to about 7.2 K. This value is equal to the difference between the temperature of maximum density of H_2O and D_2O, again considerably smaller than the value found in our study. It has also been shown that near ambient temperature, H_2O has a slightly more disordered structure than D_2O. The difference between H_2O and D_2O structure at a given temperature corresponds to the temperature-induced variation of either the H_2O or D_2O structure by a temperature shift of 5−10 K.[38,39] Furthermore, at lower temperatures, quantum effects become more pronounced.[38,39] Combined with the fact that hydrogen bonds in D_2O are expected to be stronger than in H_2O by 0.1−0.2 kcal mol^{-1}[40] and that their number generally increases with lowering temperature, this leads us to speculate that an improved understanding of the quantum mechanical nature of the hydrogen bond in a biologically relevant temperature regime (270−310 K) may help to elucidate the effects of heavy water on protein folding

DOI: 10.1021/acs.jpclett.6b00593
J. Phys. Chem. Lett. 2016, 7, 1610−1615

and phase behavior, as well as the toxicity of D_2O and its potential as an anticancer agent. The mechanisms behind this large effect of solvent isotope content on the critical point for liquid−liquid phase separation of γB-crystallin reported here are still not fully understood at this moment. Further studies into the underlying causes, as well as to establish whether this is a generic phenomenon also applying to other globular proteins, are thus clearly necessary.

EXPERIMENTAL METHODS

Following the method described by Thurston,[41] γB-crystallin was isolated and purified from fresh calf lenses, purchased from a local slaughterhouse. Final solvents with different H_2O/D_2O mixing ratios were used in this study (cf. Table 1).

SLS experiments were performed on either a home-built multiangle light scattering instrument[42] or on a commercial goniometer system (3D LS Spectrometer from LS Instruments AG[43]). SLS covers a range of scattering vectors $q = [4\pi n(\sin \theta/2)]/\lambda$ from 0.001 to 0.003 $Å^{-1}$, with θ being the scattering angle, n the refractive index of the solvent, and λ the wavelength of the radiation.

Refractive index measurements were performed on an Abbe refractometer at three different λ and extrapolated to the wavelength under consideration.

B_2 values were determined by SLS on dilute solutions using the commercial goniometer instrument at a scattering angle $\theta = 90°$.

In order to access q values much larger than those covered by SLS, we utilized the SAXS technique. Measurements were performed on a Ganesha 300 XL SAXS System from SAXSLAB with an accessible q range of 0.003−2.5 $Å^{-1}$. Data was corrected for background radiation, transmission, solvent, and capillary and was normalized with the protein concentration. The c-normalized scattering intensity is expressed as $I(q)/c \sim P(q)S(q)$, where $S(q)$ is the static structure factor and $P(q) \sim I_0(q)/c_0$ is the form factor with $P(q \to 0) = 1$. $I_0(q)$ is the measured intensity of a dilute solution (where $S(q) \approx 1$) with concentration c_0. Experimentally, the structure factors of concentrated samples are then given by $S(q) = [I(q)/c]/[I_0(q)/c_0]$.

ASSOCIATED CONTENT

Supporting Information

The Supporting Information is available free of charge on the ACS Publications website at DOI: 10.1021/acs.jpclett.6b00593.

Details of sample preparation. Details of binodal, spinodal, and second virial coefficient B_2 determination. 3D plot of full data set of Figure 4a and b. (PDF)

AUTHOR INFORMATION

Corresponding Authors

*E-mail: Najet.Mahmoudi@fkem1.lu.se.
*E-mail: Anna.Stradner@fkem1.lu.se.

Present Addresses

(L.C.-D.) Aventure AB, SE-223 63 Lund, Sweden.
(M.J.) Department of Applied Mathematics, Research School of Physical Sciences and Engineering, Australian National University, Canberra, Australian Capital Territory 2601, Australia.
(C.J.) Agroscope, Institute for Livestock Sciences ILS, CH-1725 Posieux, Switzerland.

Author Contributions

(S.B and N.M.) These authors contributed equally to this work.

Notes

The authors declare no competing financial interest.

ACKNOWLEDGMENTS

The authors thank Yuki Umehara for her help with the protein purification and sample preparation and Prof. Dr. Stefan Egelhaaf for helpful discussions. We gratefully acknowledge financial support from the Swiss National Science Foundation (SNF, grant 200020-127192), the Swedish Research Council (VR, grants 621-2012-2422 and 2009-6794), the Crafoord foundation (grants 20120619 and 20140756), and the Knut and Alice Wallenberg Foundation (project grant KAW 2014.0052).

REFERENCES

(1) Lewis, G. N.; Macdonald, R. T. Concentration of H^2 Isotope. *J. Chem. Phys.* **1933**, *1*, 341−344.
(2) Kushner, D. J.; Baker, A.; Dunstall, T. G. Pharmacological Uses and Perspectives of Heavy Water and Deuterated Compounds. *Can. J. Physiol. Pharmacol.* **1999**, *77*, 79−88.
(3) Kumar, N.; Attri, P.; Yadav, D. K.; Choi, J.; Choi, E. H.; Uhm, H. S. Induced Apoptosis in Melanocytes Cancer Cell and Oxidation in Biomolecules Through Deuterium Oxide Generated from Atmospheric Pressure Non-Thermal Plasma Jet. *Sci. Rep.* **2014**, *4*, 7589.
(4) Ikeda, M.; Suzuki, S.; Kishio, M.; Hirono, M.; Sugiyama, T.; Matsuura, J.; Suzuki, T.; Sota, T.; Allen, C. N.; Konishi, S.; et al. Hydrogen-Deuterium Exchange Effects on β-Endorphin Release from AtT20 Murine Pituitary Tumor Cells. *Biophys. J.* **2004**, *86*, 565−575.
(5) Januschowski, K.; Mueller, S.; Spitzer, M.; Schramm, C.; Doycheva, D.; Bartz-Schmidt, K.-U.; Szurman, P. Evaluating Retinal Toxicity of a New Heavy Intraocular Dye, Using a Model of Perfused and Isolated Retinal Cultures of Bovine and Human Origin. *Graefe's Arch. Clin. Exp. Ophthalmol.* **2012**, *250*, 1013−1022.
(6) Antonino, L. C.; Kautz, R. A.; Nakano, T.; Fox, R. O.; Fink, A. L. Cold Denaturation and ^2H_2O Stabilization of a Staphylococcal Nuclease Mutant. *Proc. Natl. Acad. Sci. U. S. A.* **1991**, *88*, 7715−7718.
(7) Guzzi, R.; Sportelli, L.; La Rosa, C.; Milardi, D.; Grasso, D. Solvent Isotope Effects on Azurin Thermal Unfolding. *J. Phys. Chem. B* **1998**, *102*, 1021−1028.
(8) Huyghues-Despointes, B. M. P.; Scholtz, J. M.; Pace, C. N. Protein Conformational Stabilities Can Be Determined from Hydrogen Exchange Rates. *Nat. Struct. Biol.* **1999**, *6*, 910−912.
(9) Cho, Y.; Sagle, L. B.; Iimura, S.; Zhang, Y.; Kherb, J.; Chilkoti, A.; Scholtz, J. M.; Cremer, P. S. Hydrogen Bonding of β-Turn Structure Is Stabilized in D_2O. *J. Am. Chem. Soc.* **2009**, *131*, 15188−15193.
(10) Makhatadze, G. I.; Clore, G. M.; Gronenborn, A. M. Solvent Isotope Effect and Protein Stability. *Nat. Struct. Biol.* **1995**, *2*, 852−855.
(11) Cioni, P.; Strambini, G. B. Effect of Heavy Water on Protein Flexibility. *Biophys. J.* **2002**, *82*, 3246−3253.
(12) Parker, M. J.; Clarke, A. R. Amide Backbone and Water-Related H/D Isotope Effects on the Dynamics of a Protein Folding Reaction. *Biochemistry* **1997**, *36*, 5786−5794.
(13) Efimova, Y. M.; Haemers, S.; Wierczinski, B.; Norde, W.; Well, A. A. v. Stability of Globular Proteins in H_2O and D_2O. *Biopolymers* **2007**, *85*, 264−273.
(14) Fu, L.; Villette, S.; Petoud, S.; Fernandez-Alonso, F.; Saboungi, M.-L. H/D Isotope Effects in Protein Thermal Denaturation: The Case of Bovine Serum Albumin. *J. Phys. Chem. B* **2011**, *115*, 1881−1888.
(15) Pelton, J. T.; McLean, L. R. Spectroscopic Methods for Analysis of Protein Secondary Structure. *Anal. Biochem.* **2000**, *277*, 167−176.
(16) Barth, A. Infrared Spectroscopy of Proteins. *Biochim. Biophys. Acta, Bioenerg.* **2007**, *1767*, 1073−1101.

DOI: 10.1021/acs.jpclett.6b00593
J. Phys. Chem. Lett. 2016, 7, 1610−1615

(17) Gabel, F.; Bicout, D.; Lehnert, U.; Tehei, M.; Weik, M.; Zaccai, G. Protein Dynamics Studied by Neutron Scattering. *Q. Rev. Biophys.* **2002**, *35*, 327−367.
(18) Bu, Z.; Biehl, R.; Monkenbusch, M.; Richter, D.; Callaway, D. J. E. Coupled Protein Domain Motion in Taq Polymerase Revealed by Neutron Spin-echo Spectroscopy. *Proc. Natl. Acad. Sci. U. S. A.* **2005**, *102*, 17646−17651.
(19) Schurtenberger, P. In *Neutrons, X-Rays and Light: Scattering Methods Applied to Soft Condensed Matter*; Lindner, P., Zemb, T., Eds.; Elsevier: Amsterdam, 2002; Chapter 7 (Contrast and Contrast Variation in Neutron, X-Ray and Light Scattering).
(20) Pancoska, P.; Wang, L.; Keiderling, T. A. Frequency Analysis of Infrared Absorption and Vibrational Circular Dichroism of Proteins in D_2O Solution. *Protein Sci.* **1993**, *2*, 411−419.
(21) Cavanagh, J.; Fairbrother, W. J.; Palmer, A. G. I.; Rance, M.; Skelton, N. J. *Protein NMR Spectroscopy: Principles and Practice*, 2nd ed.; Elsevier/Academic Press: Amsterdam, 2007; Chapter 3 (Experimental Aspects of NMR Spectroscopy), pp 114−270.
(22) Gripon, C.; Legrand, L.; Rosenman, I.; Vidal, O.; Robert, M. C.; Boué, F. Lysozyme Solubility in H_2O and D_2O Solutions: A Simple Relationship. *J. Cryst. Growth* **1997**, *177*, 238−247.
(23) Broutin, I.; Riès-Kautt, M.; Ducruix, A. Lysozyme Solubility in H_2O and D_2O Solutions as a Function of Sodium Chloride Concentration. *J. Appl. Crystallogr.* **1995**, *28*, 614−617.
(24) Gripon, C.; Legrand, L.; Rosenman, I.; Vidal, O.; Robert, M.; Boué, F. Lysozyme-Lysozyme Interactions in Under- and Super-Saturated Solutions: A Simple Relation Between the Second Virial Coefficients in H_2o and D_2o. *J. Cryst. Growth* **1997**, *178*, 575−584.
(25) Stradner, A.; Cardinaux, F.; Schurtenberger, P. Comment on "Effective Long-Range Attraction between Protein Molecules in Solution Studied by Small Angle Neutron Scattering". *Phys. Rev. Lett.* **2006**, *96*, 219801.
(26) Stradner, A.; Thurston, G. M.; Schurtenberger, P. Tuning Short-Range Attractions in Protein Solutions: From Attractive Glasses to Equilibrium Clusters. *J. Phys.: Condens. Matter* **2005**, *17*, S2805−S2816.
(27) Thomson, J. A.; Schurtenberger, P.; Thurston, G. M.; Benedek, G. B. Binary Liquid Phase Separation and Critical Phenomena in a Protein/Water Solution. *Proc. Natl. Acad. Sci. U. S. A.* **1987**, *84*, 7079−7083.
(28) Schurtenberger, P.; Chamberlin, R. A.; Thurston, G. M.; Thomson, J. A.; Benedek, G. B. Observation of Critical Phenomena in a Protein-Water Solution. *Phys. Rev. Lett.* **1989**, *63*, 2064−2067.
(29) Bucciarelli, S.; Casal-Dujat, L.; De Michele, C.; Sciortino, F.; Dhont, J.; Bergenholtz, J.; Farago, B.; Schurtenberger, P.; Stradner, A. Unusual Dynamics of Concentration Fluctuations in Solutions of Weakly Attractive Globular Proteins. *J. Phys. Chem. Lett.* **2015**, *6*, 4470−4474.
(30) Cardinaux, F.; Gibaud, T.; Stradner, A.; Schurtenberger, P. Interplay between Spinodal Decomposition and Glass Formation in Proteins Exhibiting Short-Range Attractions. *Phys. Rev. Lett.* **2007**, *99*, 118301.
(31) Noro, M. G.; Frenkel, D. Extended Corresponding-States Behavior for Particles with Variable Range Attractions. *J. Chem. Phys.* **2000**, *113*, 2941−2944.
(32) Gibaud, T.; Cardinaux, F.; Bergenholtz, J.; Stradner, A.; Schurtenberger, P. Phase Separation and Dynamical Arrest for Particles Interacting with Mixed Potentials - the Case of Globular Proteins Revisited. *Soft Matter* **2011**, *7*, 857−860.
(33) Platten, F.; Valadez-Pérez, N. E.; Castaneda-Priego, R.; Egelhaaf, S. U. Extended Law of Corresponding States for Protein Solutions. *J. Chem. Phys.* **2015**, *142*, 174905.
(34) Biffi, S.; Cerbino, R.; Bomboi, F.; Paraboschi, E. M.; Asselta, R.; Sciortino, F.; Bellini, T. Phase Behavior and Critical Activated Dynamics of Limited-Valence DNA Nanostars. *Proc. Natl. Acad. Sci. U. S. A.* **2013**, *110*, 15633−15637.
(35) Kleinert, H. Critical Exponents from Seven-Loop Strong-Coupling φ^4 Theory in Three Dimensions. *Phys. Rev. D: Part. Fields* **1999**, *60*, 085001.
(36) Pelissetto, A.; Vicari, E. Critical Phenomena and Renormalization-Group Theory. *Phys. Rep.* **2002**, *368*, 549−727.
(37) Lu, P. J.; Zaccarelli, E.; Ciulla, F.; Schofield, A. B.; Sciortino, F.; Weitz, D. A. Gelation of Particles with Short-Range Attraction. *Nature* **2008**, *453*, 499−503.
(38) Hart, R. T.; Mei, Q.; Benmore, C. J.; Neuefeind, J. C.; Turner, J. F. C.; Dolgos, M.; Tomberli, B.; Egelstaff, P. A. Isotope Quantum Effects in Water Around the Freezing Point. *J. Chem. Phys.* **2006**, *124*, 134505.
(39) Bergmann, U.; Nordlund, D.; Wernet, P.; Odelius, M.; Pettersson, L. G. M.; Nilsson, A. Isotope Effects in Liquid Water Probed by X-Ray Raman Spectroscopy. *Phys. Rev. B: Condens. Matter Mater. Phys.* **2007**, *76*, 024202.
(40) Scheiner, S.; Cuma, M. Relative Stability of Hydrogen and Deuterium Bonds. *J. Am. Chem. Soc.* **1996**, *118*, 1511−1521.
(41) Thurston, G. M. Liquid-Liquid Phase Separation and Static Light Scattering of Concentrated Ternary Mixtures of Bovine α- and γB-Crystallins. *J. Chem. Phys.* **2006**, *124*, 134909−10.
(42) Moitzi, C.; Vavrin, R.; Bhat, S. K.; Stradner, A.; Schurtenberger, P. A New Instrument for Time-Resolved Static and Dynamic Light-Scattering Experiments in Turbid Media. *J. Colloid Interface Sci.* **2009**, *336*, 565−574.
(43) Urban, C.; Schurtenberger, P. Characterization of Turbid Colloidal Suspensions Using Light Scattering Techniques Combined with Cross-Correlation Methods. *J. Colloid Interface Sci.* **1998**, *207*, 150−158.

DOI: 10.1021/acs.jpclett.6b00593
J. Phys. Chem. Lett. 2016, 7, 1610−1615